A real-time system for dynamic optical tomography

Christoph H. Schmitz, Harry L. Graber, Randall L. Barbour
Dept. of Pathology, SUNY Downstate Medical Center, Box 25, 450 Clarkson Ave., Brooklyn, NY 11203, U.S.A.
Tel.: 1 (718) 270-2832, Fax: 1 (718) 270-3313, Email: cschmitz@downstate.edu
Joseph M. Lasker, Andreas H. Hielscher
Depts. of Biomedical Engineering and Radiology, Columbia University, 530 West 120th St, NY, NY 10027
Yaling Pei
NIRx Medical Technologies Corp., 15 Cherry Lane, Glen Head, NY 11545, U.S.A.

Abstract: Presented are the operating characteristics of an integrated CW-near infrared tomographic imaging system capable of fast data collection and producing 2D/3D images of optical contrast features that exhibit dynamic behavior in tissue and other highly scattering media in real time. Results of preliminary *in vivo* studies on healthy and cancerous breast tissue are shown.
OCIS codes: (170.6960) Tomography; (170.5280) Photon migration

1. Introduction

Dynamic near-infrared optical tomography (DYNOT) is a new general-purpose noninvasive imaging tool capable of investigating functional states of the vasculature and its interaction with surrounding tissue structures [1,2]. In the current report, we present a description of an integrated hardware and software approach that provides for the imaging of dynamic processes in real-time. By way of example we show results obtained from a subject diagnosed with Stage II breast cancer that document altered functional states associated with the tumor vasculature.

2. Methods

2.1 Instrumentation

The concept, design rationale, and implementation of a dynamic near-infrared optical tomographic (DYNOT) imaging system have been described in recent reports [3-5]. Here we briefly summarize system functionalities.

The system currently being tested operates at two wavelengths (up to four wavelengths are possible) and features a data acquisition rate of up to ~ 2.7 full tomographic data sets per second per wavelength, (equivalent to ~ 4,300 single measurements per second). This is achieved by employing a hybrid approach of time multiplexing the source locations and frequency encoding the illuminating wavelengths. The latter allows for the parallel readout of all up to 32 detector channels at different wavelengths simultaneously. Additionally, the system employs an optical detection scheme that has an exceptionally large dynamic range (180 dB). This permits examination of large tissue volumes while maximizing the achievable data acquisition rate. The large dynamic range is achieved by an electronic gain switching scheme that automatically adjusts the sensitivity range of each detector channel in sync with the changing source location on the target.

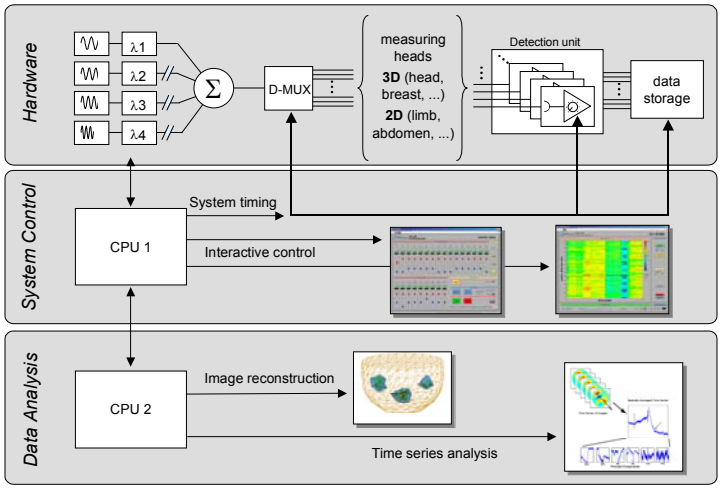

Fig. 1. Schematic of functionality and system architecture. λ1-4: lasers of different wavelengths, Σ: Overlaying beams, D-MUX: optical demultiplexer.

Other functionalities include timing hardware and a software protocol to provide communication between the system components in order to orchestrated the necessary system tasks. This includes the advancement of the source positions, the timely adjustment of the detector gain settings, and the triggering of the readout process.

Another feature of the DYNOT system is the availability of exchangeable sensor heads having various geometries that form optical interfaces suitable for a wide range

of applications. Available are sensors for the limbs (circular geometry), the breast (folding hemisphere), a helmet-like device for the head, and various two-dimensional fiber array designs for nearly planar geometries.

2.2. System operation and functionality

Fig. 1 shows a schematic of the system's architecture. The first level represents the system hardware. Indicated are the basic components that allow for the system's performance capabilities described above. The second level comprises mainly the user interface that allows for system setup and real-time viewing of acquired measurements in various formats. These are configured within a LabVIEW environment. Various display modes are available to the user, including the selection of wavelength and the display of estimated changes in blood oxygenation and volume. A third level of functionality is controlled by a second CPU, operating under a Unix environment. This provides additional levels of data processing associated with image reconstruction, image display and image analysis. Various coupled forward-inverse reconstruction algorithms are available, which allow for image recovery using first-order or recursive finite element based schemes for 2D or 3D problems. All are derived from the diffusion equation for DC illumination. Computed parameters include absorption only, scattering (diffusion) only, or both. Schemes for real-time image recovery in the case of first order solutions are described in an accompanying report by Pei *et al.* The computed image series is available for off line interrogation using a spectrum of analysis routines embedded within an interactive MATLAB environment. These allow for the computation and display of linear and nonlinear properties associated with the time-varying pixel data.

Results

Fig. 2 shows results obtained with the DYNOT system on a patient diagnosed with Stage II breast cancer. Shown are temporal changes in normalized oxy- and deoxyhemoglobin levels as estimated from a dual-wavelength measurement (760 nm and 830 nm) for a selected source-detector pair near the tumor location on the right breast and for the corresponding source-detector pair on the left (healthy breast). The indicated numbers refer to various breathing maneuvers the volunteer was asked to perform (1 = deep breathing, 2 = breath hold, 3 = recovery).

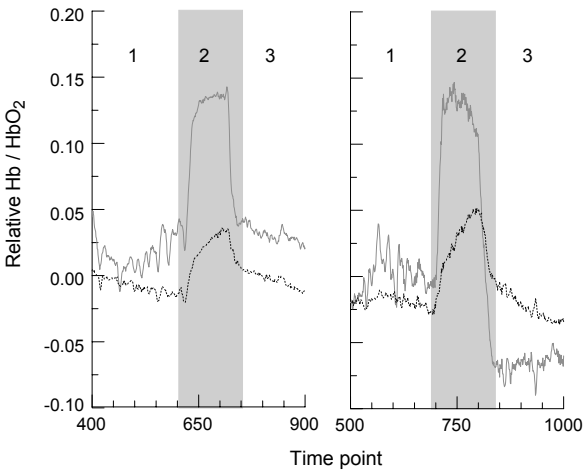

Fig. 2. Time course of hemoglobin states during a breath hold. Right: left (healthy) breast, left: right breast (w/ tumor).

Comparison between the graphs reveals a qualitatively different trend in hemoglobin states during a breath hold. In both graphs, the oxy- and deoxy-hemoglobin (HbO_2, Hb, respectively) levels rise initially upon a breath hold, which is expected because of the rise in venous return pressure will cause an increase in tissue blood volume. Following this we observe that contrary to the trend seen in the healthy breast, the HbO_2 level in the tumor bearing breast becomes unstable and then declines accompanied by a steeper rise in the levels of deoxyhemoglobin. These results are entirely consistent with the well-recognized general finding that solid tumors function on the brink of hypoxemia.

In Fig. 3 we show an example of how this information, extracted from continuous optical tomographic measurements, can serve to image tumor tissue with high contrast. Shown is an isocontour plot of the product of the time correlation values of the HbO_2 and Hb levels seen during the breath-hold computed from the 3D time-series image data. For presentation clarity, we show only those contour levels that comprise the highest 90% of the computed values (i.e., background contrast is <10% of maximum value shown). Comparison of this result to a sonogram image of the breast indicates excellent agreement. The equivalent data from the normal breast is essentially featureless for the contrast ranges shown.

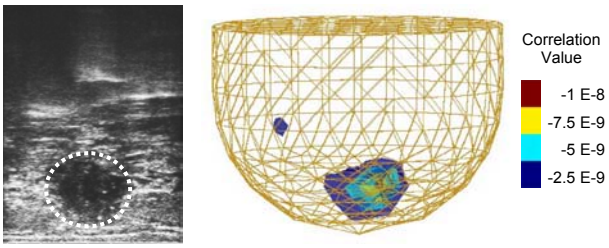

Fig. 3. Right: 3D map of correlation values for the temporal variations of oxygenation states in the tumor bearing breast. Left: Sonogram of the same breast, approx. at same scale.

3. Discussion

In this report, we have described an integrated system that is intended to serve as a general-purpose optical imaging platform for the investigation of time-varying hemoglobin states and vascular reactivity in large tissue structures. Expected application areas include use in the investigation of peripheral vascular diseases, functional brain imaging, tumor detection and its response to therapy, among others. Presented are results of a time-series imaging study performed on a tumor-bearing and tumor-free breast of a subject diagnosed with Stage II breast cancer. We have demonstrated that time correlation analysis of the variation of blood oxygenation can serve to image a tumor with high contrast.

4. References

[1]R. L. Barbour, H. L. Graber, C. H. Schmitz, Y. Pei, S. Zhong, S.-L. S. Barbour, S. B. Blattman, and T. F. Panetta, "Spatio-Temporal Imaging of Vascular Reactivity by Optical Tomography," in Proceedings of Inter-Institute Workshop on in Vivo Optical Imaging at the NIH, A. H. Gandjbakhche, ed. (Optical Society of America, Washington, DC), 161-166 (1999).

[2]R. L. Barbour, H. L. Graber, Y. Pei, S. Zhong, C. H. Schmitz, "Optical tomographic imaging of dynamic features of dense-scattering media," J. Opt. Soc. Am. A, **18**, pp. 3018–3036 (2001).

[3]C. H. Schmitz, H. L. Graber, H. Luo, I. Arif, J. Ira, Y. Pei, A. Bluestone, S. Zhong, R. Andronica, I. Soller, N. Ramirez, S.-L. S. Barbour, and R. L. Barbour, "Instrumentation and calibration protocol for imaging dynamic features in dense-scattering media by optical tomography," Appl. Opt., **39**, 6466-6485 (2000).

[4]C. H. Schmitz, M. Löcker, J. M. Lasker, A. H. Hielscher, R. L. Barbour, "Instrumentation for fast functional optical tomography," Rev. Sci. Instr., in press (2002).

[5]C. H. Schmitz, Y.Pei, H. L. Graber, J. M. Lasker, A. H. Hielscher, R. L. Barbour, "Instrumentation for Real–Time Dynamic Optical Tomography," Proc. SPIE, **4431**, pp. 282–291 (2001).

5. Acknowledgements

This research was supported by NIH grants RO1–CA 66184 (RLB), R01 AR46255–01 (AHH), and the NYC Council Speaker's Fund for Biomedical Research: Towards the Science of Patient Care (AHH).